nature reviews physics

https://doi.org/10.1038/s42254-025-00869-7

Review article

Check for updates

Artificial gauge fields in photonics

Wange Song[1,2] ✉, Yi Yang[2,3], Zhiyuan Lin[1], Xuanyu Liu[1], Shengjie Wu[1], Chen Chen[1], Yongguan Ke[4,5], Chaohong Lee[4,6], Wei Liu[7] ✉, Shining Zhu[1], Yuri Kivshar[8] ✉, Tao Li[1] ✉ & Shuang Zhang[2,6,9,10,11] ✉

Abstract

Structured photonic systems, from photonic crystals to metamaterials and metasurfaces, provide a broad platform for photonic gauge fields. This artificial version of the real gauge fields in electrodynamics can induce a range of exotic functionalities in many branches of optical physics, enabling the manipulation of light and its interactions with various photonic structures in new and interesting ways. In this Review, we provide a viewpoint on how the concept of artificial gauge fields can connect seemingly unrelated optical effects. Artificial gauge fields in photonics can be either vectorial or scalar, Abelian or non-Abelian, real or complex. They apply not only to conventional real and momentum spaces, but also to spaces spanned by other synthetic dimensions, and are applicable to both semiclassical and quantum systems. In this Review, leveraging the wide applicability of the artificial gauge field, we connect different optical branches, including topological photonics, non-Abelian physics and non-Hermitian photonics. We discuss the current progress and next steps of research on optical gauge fields as well as their potential for future applications.

Sections

Introduction

Abelian gauge fields

Non-Abelian gauge fields

Complex gauge fields

Artificial gauge fields for quantum electrodynamics

Challenges and further applications

[1]National Laboratory of Solid State Microstructures, Key Laboratory of Intelligent Optical Sensing and Manipulations, Jiangsu Key Laboratory of Artificial Functional Materials, Collaborative innovation center of advanced microstructures, College of Engineering and Applied Sciences, Nanjing University, Nanjing, China. [2]New Cornerstone Science Laboratory, Department of Physics, University of Hong Kong, Hong Kong, China. [3]HK Institute of Quantum Science and Technology, University of Hong Kong, Hong Kong, China. [4]Institute of Quantum Precision Measurement, State Key Laboratory of Radio Frequency Heterogeneous Integration, College of Physics and Optoelectronic Engineering, Shenzhen University, Shenzhen, China. [5]Laboratory of Quantum Engineering and Quantum Metrology, School of Physics and Astronomy, Sun Yat-Sen University (Zhuhai Campus), Zhuhai, China. [6]Quantum Science Center of Guangdong–Hong Kong–Macao Greater Bay Area, Shenzhen, China. [7]Nanhu Laser Laboratory and Hunan Provincial Key Laboratory of Novel Nano-Optoelectronic Information Materials and Devices, College for Advanced Interdisciplinary Studies, National University of Defense Technology, Changsha, P. R. China. [8]Nonlinear Physics Center, Research School of Physics, Australian National University, Canberra, Australian Capital Territory, Australia. [9]Department of Electronic and Electrical Engineering, University of Hong Kong, Hong Kong, China. [10]Materials Innovation Institute for Life Sciences and Energy (MILES), HKU-SIRI, Shenzhen, China. [11]State Key Laboratory of Optical Quantum Materials, The University of Hong Kong, Hong Kong, China. ✉e-mail: songwange@nju.edu.cn; liuwei09d@nudt.edu.cn; yuri.kivshar@anu.edu.au; taoli@nju.edu.cn; shuzhang@hku.hk

Key points

- Artificial gauge fields, stimulated by concepts of topology, singularity, non-Hermiticity and non-Abelian character, have become a unifying framework that permeates and connects diverse branches of photonics.
- Artificial gauge fields bridge vibrant fields of research in optics and photonics across both classical and quantum systems.
- Artificial gauge fields provide a versatile platform to explore fundamental physics and develop advanced photonic devices, which may include integrated photonic circuits.

Introduction

Gauge fields, initially introduced as a mathematical reformulation of classical electrodynamics[1], have now evolved into a broadly applicable concept in physics. These fundamental fields ensure gauge invariance — symmetry under local transformations — and serve as a unifying concept across diverse areas of physics, from high-energy physics and cosmology to condensed matter physics[2]. The physical consequence of gauge fields is most noticeably evidenced by the Aharonov–Bohm effect[3], where charged particles experience a phase shift in regions with zero electric and magnetic fields, driven solely by electromagnetic vector potentials. With the development of quantum field theory, gauge fields have been recognized as the mediator fields associated with the fundamental forces, reformulated through phase factors[4].

Fundamental neutral particles without spin magnetic moments are generally immune to electromagnetic forces and thus also to the real gauge potentials that are associated with electromagnetic fields. One can apply external spatial or temporal modulations to construct artificial gauge fields to control neutral particles — including photons — in a manner that is equivalent to how real gauge fields affect charged particles. Artificial gauge fields have been realized in various physical systems, ranging from ultracold atomic gases[5,6] and photonics[7,8] to optomechanics[9], mechanics[10], acoustics[11] and electrical circuits[12]. Artificial gauge fields bridge different communities, enabling the study of fundamental physics as well as the invention of devices for flexible manipulation of various types of waves.

The area of artificial gauge fields is progressing swiftly, particularly in photonics, owing to the multitude of effects that gauge potentials allow. In this Review, we illuminate the notion of artificial gauge fields and demonstrate how this unifying concept threads through some of the most vibrant research areas in optics and photonics, including transformation optics[13], supersymmetry (SUSY) in optics[14], topological photonics[15–17], non-Abelian optics[18], non-Hermitian photonics with parity–time (PT) symmetry[19–22] and skin effects[23,24]. These disciplines differ in character: they can be either scalar or vectorial, Abelian or non-Abelian, real or complex, using classical or quantum systems[25,26] (see Fig. 1). To avoid confusion, we emphasize that generally the terminology of gauge fields is a comprehensive concept that encompasses both gauge potentials (such as scalar and vector potentials in electromagnetism) and their derivative fields, such as electromagnetic fields **E** and **B** (ref. 27; see Wu-Yang Dictionary in ref. 4). However, in a more specific and narrow sense, gauge fields is sometimes used only for the derivative fields. In this Review, we adopt the broad term of artificial gauge fields that encompasses both gauge potentials and their derivative fields.

In this Review, we first provide an overview of conventional artificial gauge fields, divided into two subsections. The first of these discusses spatial engineering of scalar potentials for light manipulation; the second addresses vector potentials, both rotational and irrotational, which underpin various phenomena in topological photonics and enable versatile light control. We then examine non-Abelian gauge fields with non-commutative, matrix-valued gauge potentials. The next section extends the discussion from real to complex domains, focussing on gauge potentials in non-Hermitian systems. Finally, we provide a concise overview of artificial gauge fields in quantum systems and discuss challenges and further applications of artificial gauge fields.

Abelian gauge fields

Scalar gauge potentials

The scalar gauge potential, which originates from the gauge transformation of the electromagnetic field, corresponds to the electric potential and is exemplified by the electric Aharonov–Bohm effect[3], which shares its underlying mechanism with the Mach–Zehnder interferometer. Optical scalar gauge potentials can be obtained through engineering the refractive index profile of the medium, inducing additional phases for the propagating photons (see Box 1). The development of nanofabrication technologies has made photonic structures with desired refractive index distributions possible, and thus flexible modulations of scalar gauge potential in one or more spatial dimensions can be achieved. Examples include waveguide lattices, photonic crystals, plasmonics, metamaterials and metasurfaces. Gauge fields provide a practical degree of freedom that promotes abundant manipulations of light and has inspired many research directions in photonics.

Adjusting the refractive index of a photonic lattice corresponds to applying a bias to regulate the motion of electrons in a crystal lattice. For example, the introduction of external static electric fields in a crystal results in an oscillatory motion of electrons, known as Bloch oscillations[28,29], which are another type of scalar gauge potential (electric field) application. A parallel concept exists in photonics — optical Bloch oscillations. Here, a transverse refractive index gradient mimics a static electric field (Fig. 2a), and the optical Bloch oscillations can be directly observed as an oscillatory beam along the propagation direction[30,31]. Besides optical Bloch oscillations originating from a linear gradient of scalar potential, applying parabolic potentials can generate polychromatic bouncing plasmonic waves[32] and realize focusing of optical beams[33]. The scalar gauge potential can also be periodically modulated along the longitudinal direction (Fig. 2b). At a certain resonant modulation frequency, the coupling between neighbouring waveguides can be suppressed owing to phase modulation, which inhibits light tunnelling[34]. Recently, bimorphic Floquet topological insulators have been realized by leveraging connective chains with periodically modulated propagation constants, revealing rich topological phases in a Floquet honeycomb lattice without resorting to magnetic interactions[35].

In addition to smoothly modulating the magnitude of scalar potentials, one can control light propagation by rearranging or reordering these potentials in real space. For example, deformations in the host lattice have been applied to implement non-trivial topological states[36] (Fig. 2c). These deformations are characterized by real-space topology and cannot be eliminated by local continuous transformations. Disclination structures, formed by 'cutting and gluing' a host lattice, are representative of such topological deformations[37,38]. A photonic disclination lattice based on a two-dimensional (2D) Su–Schrieffer–Heeger lattice successfully achieved robust transport of an optical vortex with

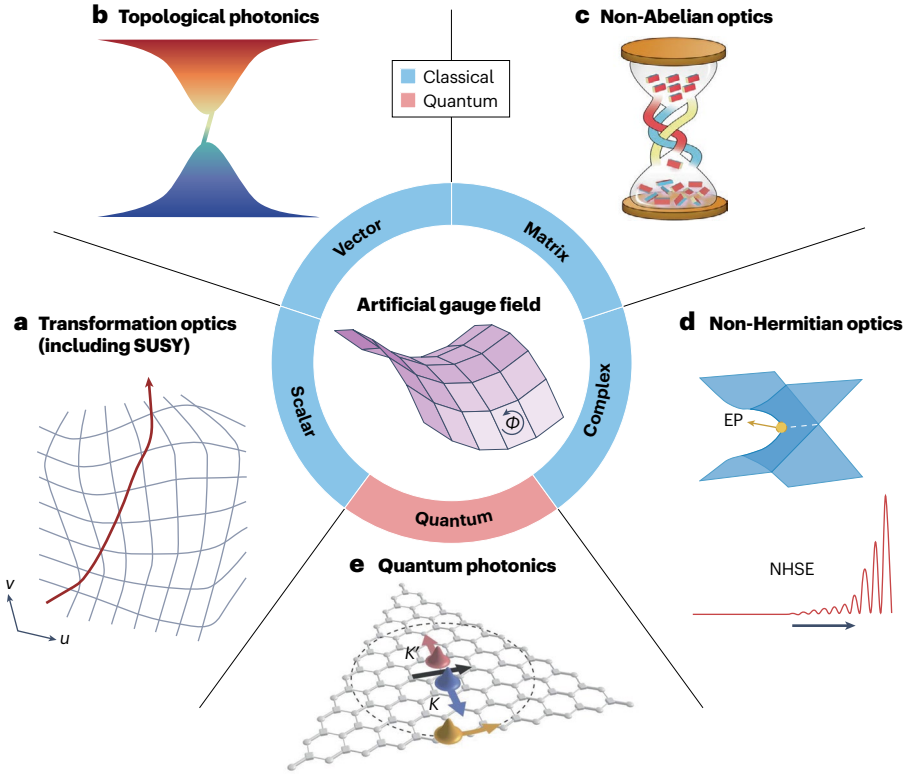

Fig. 1 | Artificial gauge fields in photonics. Artificial gauge fields show varying levels of complexity in photonics, ranging from scalar to vectorial, Abelian to non-Abelian, and real to complex, underlying various research areas in optics and photonics across both classical (blue) and quantum (pink) systems. **a**, Transformation optics including supersymmetry (SUSY). A distorted field line (red), representing a light ray, is shown alongside the background coordinate grid (grey) deformed in the same manner. **b**, Topological photonics. A representative band structure of a topological insulator, illustrating the emergence of topological edge states within the bulk bandgap. **c**, Non-Abelian optics, illustrated by an hourglass of non-Abelian physics, featuring three passages each transporting a distinct degree of freedom along the braiding pathway from an ordered to a disordered phase. **d**, Non-Hermitian photonics. Top, a typical band structure for non-Hermitian systems featuring an exceptional point (EP). Bottom, manifestation of the non-Hermitian skin effect (NHSE), where all bulk eigenstates become localized at a boundary. **e**, 2D Fock-state lattices showing a valley Hall response, for which wavepackets at two valleys move in opposite directions, perpendicular to an applied force (black arrow), and Haldane chiral edge states (yellow wavepacket and arrow). Part **a** reprinted with permission from ref. 13, AAAS. Part **b** adapted from ref. 17, Springer Nature Limited. Part **c** adapted with permission from ref. 18, AAAS. Part **d** adapted with permission from ref. 22, AAAS. Part **e** adapted with permission from ref. 26, AAAS.

preserved orbital angular momentum[39]. Another example is fractal geometries. Recently, there has been growing interest in exploring fractals within the framework of topological insulators, using photonic lattices. The most intriguing aspect is that, despite not having an actual bulk, fractal lattices can sustain topological chiral edge states[40,41] (Fig. 2d). Besides the disclinations and fractals just mentioned, other types of topological deformations include dislocations, Dirac vortices and moiré lattices[36].

The above examples require specific modulations of scalar gauge potential to demonstrate specific effects or functionalities. To describe and control the behaviour of light propagation with high precision in a more general manner, a powerful mathematical technique called transformation optics helps to design artificial optical materials and devices with spatially customized optical properties[13] (Fig. 2e). The desired transformations often require extreme material parameters, making experimental realizations challenging. A concept called supersymmetry (SUSY), originally proposed in quantum field theory, has been introduced to photonics[14] (Fig. 2f). It provides a new perspective for transformation optics to design scalar potentials to arbitrarily steer and switch the flow of light[42,43]. By coupling a main structure with a SUSY partner, it is possible to substantially reduce the threshold of the desired mode relative to other modes and achieve a high-power single-mode laser array[44]. The SUSY modulations can also control the optical scattering characteristics[42], realizing mode division multiplexing[45] and manipulating the excitation and evolution of topological states[46].

Vector gauge potentials

The vector gauge potential (VGP) corresponds to the magnetic vector potential in electrodynamics and is related to the well-known magnetic Aharonov–Bohm effect[3]. The artificial VGP can generate coupling of complex values between neighbouring waveguides after gauge transformation (see Box 1). The VGP provides an effective approach to induce a non-reciprocal response for light. In particular, it serves as the fundamental mechanism underlying many topological phenomena through its effective **B** fields ($\mathbf{B} = \nabla \times \mathbf{A}$). Over the past 20 years, the concept of topology that characterizes the global overall behaviour of wavefunctions has provided an extra degree of freedom for wave

Box 1 | Artificial gauge potentials in photonics

Artificial gauge potentials can be introduced into photonic systems by exploiting additional parameter spaces. The parameters used can be internal (such as the spin and orbital dimensions of photons) and/or external (spatial or temporal modulations of the photonic properties). Here we discuss the basic concept of artificial gauge fields using the example of photonic waveguide lattices. We consider the simplest scenario of paraxial wave propagation in a waveguide lattice[8], where the waveguide axes are spatially modulated as $x=x_a(z)$ and $y=y_a(z)$ (see panel **a**).

Within the paraxial approximation, light propagation can be described by a Schrödinger-type equation in the laboratory reference frame $i\partial_z\psi(x,y,z)=H\psi(x,y,z)$ with the Hamiltonian $H=-\frac{1}{2k_0}\nabla_\perp^2-\frac{k_0}{n_0}\Delta n(\mathbf{r})$, where $\nabla_\perp^2$ is the Laplacian implemented on the transverse plane; $\mathbf{r}=x\hat{\mathbf{x}}+y\hat{\mathbf{y}}+z\hat{\mathbf{z}}$ is the spatial position vector ($\hat{\mathbf{x}}$, $\hat{\mathbf{y}}$ and $\hat{\mathbf{z}}$ are unit vectors); $k_0=2\pi n_0/\lambda$ (λ being the free-space wavelength) is the wavenumber in the ambient medium of index n_0; $\Delta n(\mathbf{r})$ is the spatial index modulation in the ambient medium. Light propagation can be viewed as unmodulated if it is transformed from the laboratory reference frame to the waveguide reference frame $x'(z)=x-x_a(z)$, $y'(z)=y-y_a(z)$, $z'=z$. In the new coordinates, light evolution can then be described by the transformed Hamiltonian:

$$H'=-\frac{1}{2k_0}(\nabla_\perp'-i\mathbf{A})^2-\Phi-\frac{1}{2k_0}\mathbf{A}^2 \quad (1)$$

where $\mathbf{A}=k_0[\partial x_a(z)/\partial z\hat{\mathbf{x}}+\partial y_a(z)/\partial z\hat{\mathbf{y}}]$ is the associated artificial vector gauge potential (VGP) and $\Phi=k_0\Delta n/n_0$ is the artificial scalar gauge potential (SGP) (panel **a** of the figure).

Adopting the tight-binding approximation, in which the mode of a waveguide lattice can be written as a weighted sum of the individual waveguide modes $\psi(\mathbf{r})=\sum_m a_m(z)\phi_m(x,y)$, where $\phi_m(x,y)$ is the transversal waveguide mode function for the mth waveguide and $a_m(z)$ is the modal coefficient. The Schrödinger equation now becomes the coupled-mode equation $\sum_m a_m(z)c_{mn}=i\frac{\partial}{\partial z}a_n(z)$, where $c_{m,n}$ is the coupling coefficient between mth and nth waveguides. To reveal the role of such gauge potentials in the evolution of light in the waveguide lattice, we apply a gauge transformation similar to that in electrodynamics: $\phi'(x,y)=\phi(x,y)\exp(i\theta)$, where $\theta=\int_r\mathbf{A}\cdot d\mathbf{r}+\int_z\Phi dz$ is the phase originating from the artificial potentials. The gauge potential modulates the coupling between two lattice sites:

$$c_{mn}^{VGP}=c_0\exp(i\mathbf{A}\cdot\mathbf{R}_{mn}),\ c_{mn}^{SGP}=c_0\exp(i\Delta\varphi_{mn}) \quad (2)$$

where c_0 is the original coupling coefficient, $\mathbf{R}_{mn}$ is the relative-position vector between mth and nth sites, and $\Delta\varphi_{mn}=-\int_z(\Phi_m-\Phi_n)dz$. Both the SGP and VGP can induce different phases for opposite coupling directions, $\theta_R=-\theta_L$. We emphasize that the extra gauge-potential-induced phase factors for the coupling coefficients each have a distinct nature: the VGP phase factor $\exp(i\mathbf{A}\cdot\mathbf{R}_{mn})$ manifests a typical geometric phase feature (not accumulated along z) whereas the SGP phase factor $\exp(i\Delta\varphi_{mn})$ is intrinsically dynamic (panels **b** and **f**).

Owing to the commutative nature of scalars and vectors (first-order tensors), the extra phase factors can retrace their path back to the origin along the opposite route. That is to say, the artificial gauge potentials that we have described so far are Abelian. The lowest-order non-Abelian gauge potentials (SU(2)) can be obtained by simply replacing the basis vectors of the VGP and SGP with matrices:

$$\mathbf{A}=\sum_{j=1}^{3}A^j\sigma_j,\ \Phi=\sum_{j=1}^{3}\Phi^j\sigma_j \quad (3)$$

where σ_j (j=1,2,3) are Pauli matrices. This extension can accommodate extra degrees of freedom for the system investigated. For example, within photonic lattices, the propagation of vectorial waves (with non-negligible polarization effects) can be described by the non-Abelian model. In the context of non-Abelian gauge potentials, the accumulation of the phase θ is no longer commutative. Consequently, both the coupling coefficients and onsite potentials become matrix valued (panels **c** and **g**).

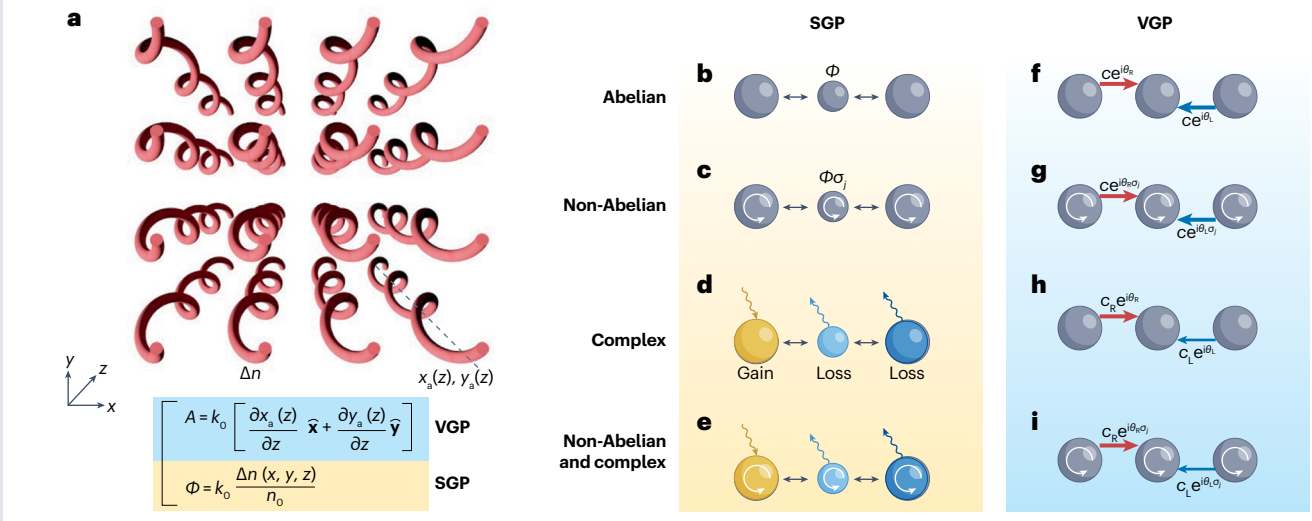

(continued from previous page)

Moreover, the gauge potentials discussed above do not have to be real: for example $\mathbf{A}=\mathbf{A}_r+i\mathbf{A}_i$ where $\mathbf{A}_r$ and $\mathbf{A}_i$ are real. Complex VGPs modulate not only the phase but also the amplitude of the coupling coefficients, that is, $c_{mn}=c_0\exp(i\mathbf{A}_r\cdot\mathbf{R}_{mn})\exp(-\mathbf{A}_i\cdot\mathbf{R}_{mn})$, and then the coupling strength is

$$|c_{mn}| = |c_0|\exp(-\mathbf{A}_i\cdot\mathbf{R}_{mn}) \quad (4)$$

Equation (4) shows that a complex VGP leads to asymmetric couplings, $c_R=|c_{mn}|\neq|c_{nm}|=c_L$. For an SGP, we can replace the real index n with the complex index $n=n_r+in_i$, where n_i corresponds to the gain or loss of the material, making the SGP complex (panel **d** and **h**). Complex gauge potentials can also be combined with the non-Abelian gauge potentials (panels **e** and **i**).

manipulation in photonic systems. This field hinges on the calculation of a topological invariant within the bulk of a crystal, which, through bulk–boundary correspondence, predicts boundary-localized states. For a comprehensive understanding of the fundamental concepts in topological photonics, we refer the reader to existing reviews[15–17].

The quantum Hall effect, associated with broken time-reversal symmetry, was one of the first phenomena in which observable physical effects caused by momentum-space topology were identified[47]. Its physical origin lies in the energy band structure, with the Berry curvature playing a role analogous to the real magnetic field in real space (Fig. 3a). This correspondence enables the quantum Hall effect to be observed with light by engineering the band structure of photonic crystals with non-zero Chern numbers[48,49], as experimentally realized in a magneto-optical photonic crystal in the microwave regime[50]. However, this method is not widely applicable, especially for optical frequencies, at which the magnetic response is intrinsically weak.

An alternative approach to introduce a VGP is through temporal modulations of photonic crystals, which breaks time-reversal symmetry and produces one-way edge states[7]. Experimentally, this idea can be realized by Floquet-engineering the photonic lattice along the propagation direction with coupled helical waveguides[8] (Fig. 3b). After a gauge transformation, a vector potential appears in the coupling phase, which can be interpreted as the result of a circularly rotating reference frame (the mechanical analogue is the Coriolis force ($\propto\mathbf{v}\times\boldsymbol{\Omega}$), which is analogous to the magnetic Lorentz force ($\propto\mathbf{v}\times\mathbf{B}$)). The induced VGP breaks time-reversal symmetry (z-reversal symmetry as z simulates the temporal coordinate t), leading to photonic Floquet topological insulators. A similar structure with straight waveguides rather than helical ones, inspired by carbon-based graphene, was proposed to create a strain-induced pseudo-magnetic field[51]. The concept of strain-engineered artificial gauge fields has also been exploited in a 2D acoustic structure that supports airborne acoustic waves[52]. Furthermore, from the perspective of artificial gauge fields, smooth chiral strain-engineering has been proposed to obtain localized photonic edge states with tunable capability[53].

There are also proposals for an optical analogue of the quantum spin Hall effect[54,55]. In these systems, the time-reversal symmetry is preserved and photons with opposite spins encounter an effective magnetic gauge field in opposite directions. Consequently, the edge modes of opposite spins move in opposite directions. Additional topological configurations that maintain time-reversal symmetry have been proposed in the context of valley Hall topological insulators, characterized by spin-dependent in-gap edge states[56,57]. In addition, based on dynamic modulation of the photonic system, effective gauge potentials can be introduced to create a photonic Aharonov–Bohm effect, enabling non-magnetic optical isolation on chip[58]. Recently, an optical Trojan light beam was successfully demonstrated, in which guiding of the light is induced by an effective vector potential created by a heated helical iron wire, in an optical analogue of the way that Lagrange points trap celestial objects via the Coriolis force[59].

In addition to momentum-space and real-space manipulations, the concept of VGPs can be generalized and extended to synthetic dimensions (other degrees of freedom besides position or momentum)[60,61], such as frequency[62], spatial or temporal modes[63,64], or orbital angular momentum[65]. Combinations of synthetic dimensions and real space offer versatile modulation of the degrees of freedom. A wide variety of physics, including topological edge currents, has been observed in a single photonic cavity with the incorporation of synthetic frequency and pseudospin dimensions[66] (Fig. 3c). Besides this, parameters in a Hamiltonian can be treated as synthetic momenta, allowing the observation of high-dimensional physics using the topological pumping process[67,68], of synthetic Weyl degeneracies in 3D[69,70], and of topology beyond the three real dimensions[71,72]. For a comprehensive account of synthetic dimension topology, we refer the reader to a existing review that details approaches to constructing synthetic dimensions and the resulting key physical phenomena[61].

Even if the associated magnetic field $\mathbf{B}$ vanishes, one can still expect intriguing transport dynamics of photons originating from the underlying VGP. Such curl-less VGPs ($\mathbf{B}=\nabla\times\mathbf{A}=0$, $\mathbf{A}\neq0$) can modify the dispersion of an artificial structure in momentum or synthetic space, thereby altering the responses of photons. For example, negative refraction can be realized in twisted bilayer metamaterials, where the relative rotation of the two layers can induce a uniform VGP, forcing a medium to display negative refraction effects[73] (Fig. 3d). In photonics, effective gauge potentials can be achieved by tilting the optical waveguide arrays, adjusting the dispersion curves in the core and cladding, thereby restricting the light to the core[74] (Fig. 3e). Recently, photonic crystal fibres that enable topological light confinement and guiding have been theoretically proposed[75] and experimentally demonstrated[76,77]. These fibres show intriguing properties, such as much lower bending losses, and offer opportunities for optical communications. If this multilayer stacking of different gauge potentials is replaced by a longitudinal cascading form, one can expect superlens imaging functionality[78]. In this scenario, the gauge potentials induce effective negative couplings between the waveguides, equivalent to a negative refractive index, so that light incident from the positive coupling region will be focused in the negative coupling region, which resembles a superlens[79].

Scalar and vector potentials are widely considered separately for manipulation of light, and simultaneous exploitation of both potentials in a single system remains rare. Recent reports have highlighted the capability to reconfigure refraction manipulations at synthetic temporal interfaces using both SGPs and VGPs[80], verifying the ability to manipulate gauge potentials in temporal lattices[81]. This is a promising start to investigating the joint physical effects[82] resulting from simultaneously using multiple gauge potentials (Fig. 3f).

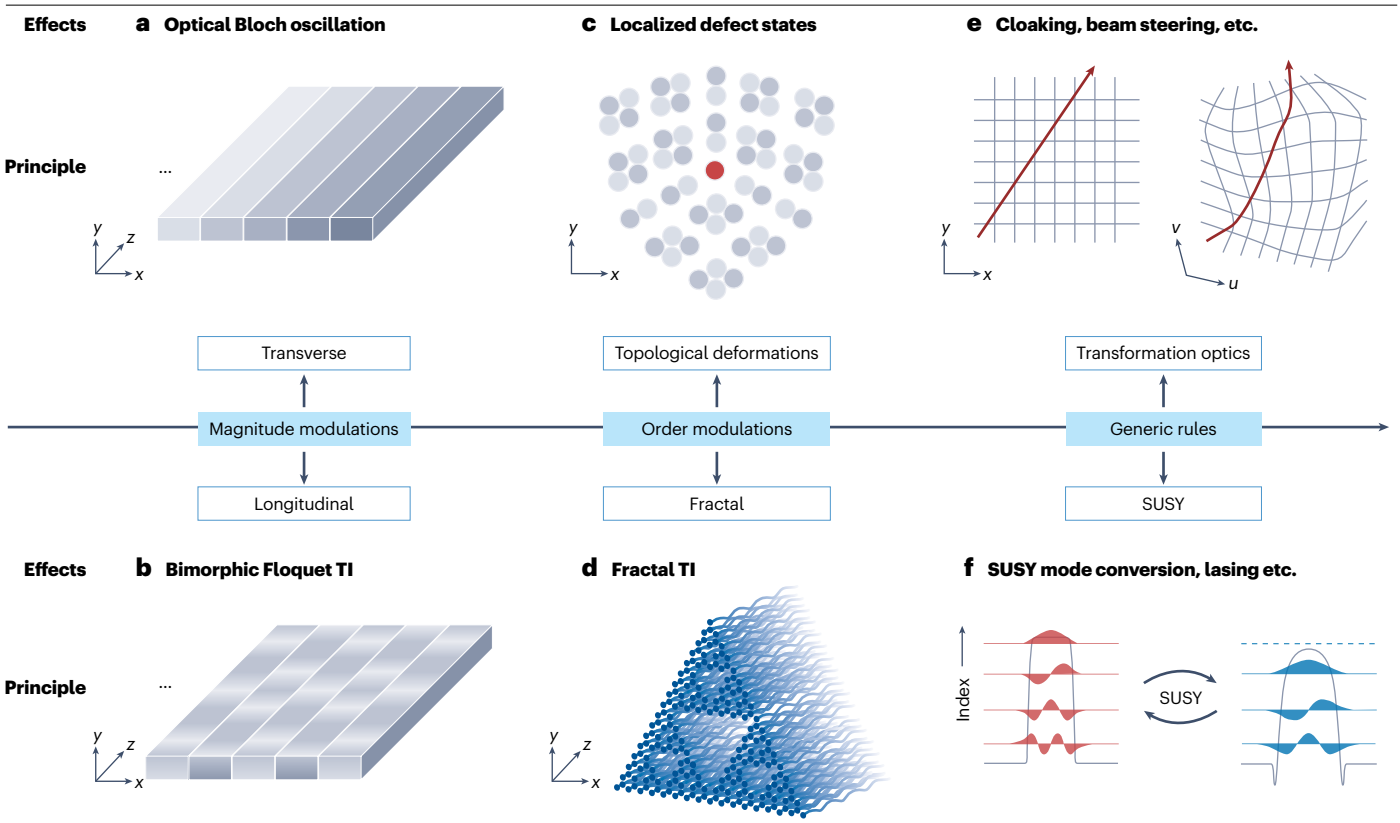

Fig. 2 | Scalar gauge potentials. a,**b**, Schematic view of optical waveguide array with transverse (panel **a**) and longitudinal (panel **b**) magnitude modulation of scalar potentials, where the shade represents the intensity of the potential. These two modulations can give rise to optical Bloch oscillations and bimorphic Floquet topological insulators (TIs), respectively. **c**,**d**, Illustration of order modulations of scalar potentials, including topological deformations supporting localized defect states (panel **c**) and fractal TI (panel **d**)[41]. **e**,**f**, Schematic representation of transformation optics (panel **e**)[13] and supersymmetric (SUSY) transformation (panel **f**)[45]. In transformation optics (panel **e**), light rays (red) can be bent by applying coordinate transformations (grey net) to the electromagnetic space. In the SUSY transformation using multimode waveguides (panel **f**), all the propagation constants of modes of the superpartner structure (right) are perfectly matched to higher-order modes of the original waveguide (left). Part **d** reprinted with permission from ref. 41, Optica. Part **e** reprinted with permission from ref. 13, AAAS. Part **f** reprinted from ref. 45, Springer Nature Limited.

Hybrid use of different gauge potentials will endow physical systems with a broad spectrum of unique characteristics that are inherently elusive, such as tunable temporal cloaking[81] and the observation of Landau–Zener tunnelling[82], enabling highly flexible and precise manipulation of light.

Non-Abelian gauge fields

The artificial gauge fields discussed above belong to the U(1) gauge field, whose states form a circle in the Hilbert space (Fig. 4a, left panel). All rotations on the circle are commutative, resulting in Abelian geometric phases. Additional intrinsic degrees of freedom can be used to construct non-Abelian gauge fields. For example, distinct spin states spanning the Bloch sphere are associated with the SU(2) gauge field[83] (Fig. 4a, right panel). These non-Abelian gauge fields, with their degenerate states in the underlying Hilbert space, lead to non-commutative rotations around different axes, which can be described by the non-commutative Pauli matrices or quaternions[84].

In photonics, non-Abelian gauge fields involve an additional commutator term concerning the potentials[85], with matrix-valued vector and scalar potentials (see Box 1). Consequently, the uniform potentials in non-Abelian systems can give rise to non-zero synthetic magnetic or electric fields, induced by extra spin-like degrees of freedom. Their existence has been confirmed through phenomena such as Zitterbewegung – a trembling motion caused by wave interference of quasidegenerate modes[86–89] – and non-Abelian Aharonov–Bohm interference[83,86,90]. Photonic systems have advantages when constructing non-Abelian gauge fields. Below, we summarize several typical approaches for generating non-Abelian gauge fields in photonics, including anisotropic media, spin–orbit interaction of polaritons, and non-reciprocal loops that break time-reversal symmetry.

In a homogeneous anisotropic medium that shows electromagnetic duality, the corresponding electromagnetic wave equation features non-Abelian vector and scalar potentials, which enable the construction of non-Abelian gauge fields[86]. By manipulating the permittivity and permeability of the medium, it is possible to generate effective magnetic or electric fields. This causes Zitterbewegung in a homogeneous medium (Fig. 4b). Moreover, two distinct media with different effective non-Abelian gauge fields can each form a loop in real space. If two coherent light beams of an identical polarization traverse the paths in opposite sequences, they will ultimately exhibit distinct

final polarizations. This corresponds to the SU(2) field and gives rise to non-Abelian Aharonov–Bohm interference, which is different from the commutative evolution of states in an Abelian field.

Non-Abelian gauge fields can also be realized by polaritons in optical microcavities or photonic crystals, leading to an optical analogue of spin–orbit coupling[87,91] where the splitting of degenerate spin states can be expressed as the splitting of TE–TM modes. In planar optical microcavities, one can construct an effective Hamiltonian with a Rashba-type spin–orbit coupling term, simulating the Yang–Mills Lagrangian[85]. Such a Hamiltonian can describe the motions of light and particles with pseudospins, predicting the Zitterbewegung of polaritons[87,91] and the lensing effect in the presence of defects[87] (Fig. 4c). Dresselhaus-type spin–orbit interactions can be implemented in a honeycomb microcavity lattice, in which the spin Hall effect associated with non-Abelian gauge fields has been observed[92].

The two approaches discussed above for constructing non-Abelian gauge fields either use the intrinsic properties of the medium or the excitation modes of polaritons. Additionally, the non-Abelian gauge fields can be endowed with flexible tunability by using tunable fibre-optic systems[83]. Using electro-optic temporal modulation and the Faraday effects to break time-reversal symmetry, one can introduce effective Pauli σ_z-type and σ_y-type fields to create non-reciprocal loops, enabling non-Abelian Aharonov–Bohm interference with multiple controllable degrees of freedom (Fig. 4d). In addition, non-Abelian gauge fields can emerge from dynamic evolutions in parameter space, as seen in non-Abelian Thouless pumps with degenerate bands. These pumps have

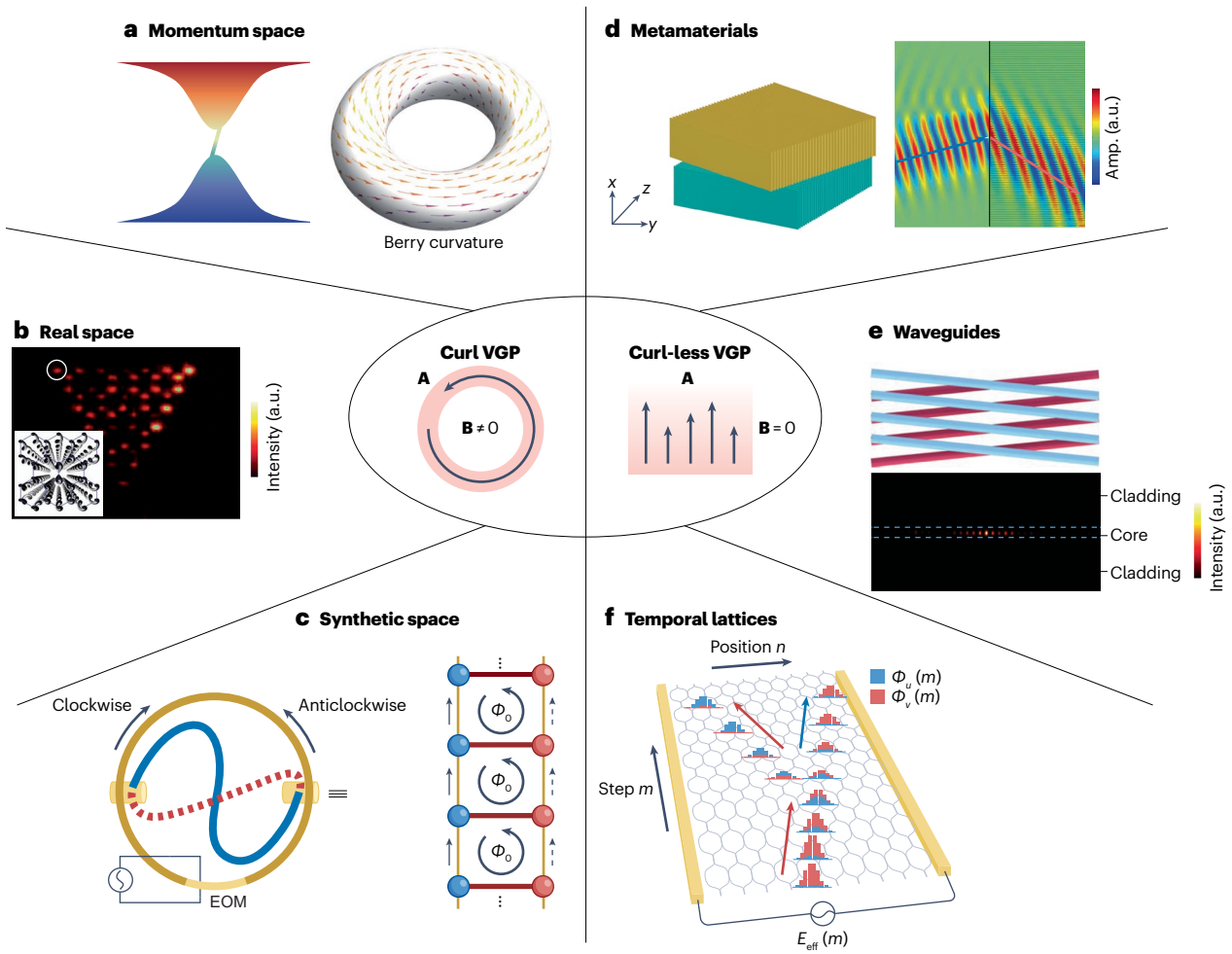

Fig. 3 | Vector gauge potentials. a, A plot of non-trivial topological band structure (left) and the Berry curvature (right; effective magnetic field in momentum space)[17]. The integral of the Berry curvature over the Brillouin zone — a torus in two dimensions — yields a non-trivial topological invariant, resulting in the appearance of protected edge states in the bulk bandgap, as shown in the left panel. **b**, Helical waveguides (inset sketch) featuring artificial gauge fields in real space (main panel), with corresponding topological modes propagating along the boundary[8]. **c**, An electro-optic modulated (EOM) ring resonator (left) and its corresponding lattice with modulated gauge potentials (ϕ_0) in synthetic dimensions formed by the clockwise and anticlockwise modes (right)[66]. **d**, Perspective view of metamaterials with different gauge potentials (left), demonstrating negative refractions — the wave refracts on the same side of the normal as the incident wave (right)[73]. **e**, Tilting of optical waveguides (top) can induce an artificial gauge field, resulting in light-guiding functions (bottom)[74]. **f**, Illustration of synthetic temporal lattices with modulated vector and scalar gauge potentials showing Landau–Zener tunnelling effects, as indicated by the wavepacket splitting[82]. VGP, vector gauge potential. Part **a** adapted from ref. 17, Springer Nature Limited. Part **b** adapted from ref. 8, Springer Nature Limited. Part **c** reprinted with permission from ref. 66, AAAS. Part **d** is adapted from ref. 73, CC BY 4.0. Part **e** is adapted from ref. 74, CC BY 4.0. Part **f** is adapted from ref. 82, CC BY 4.0.

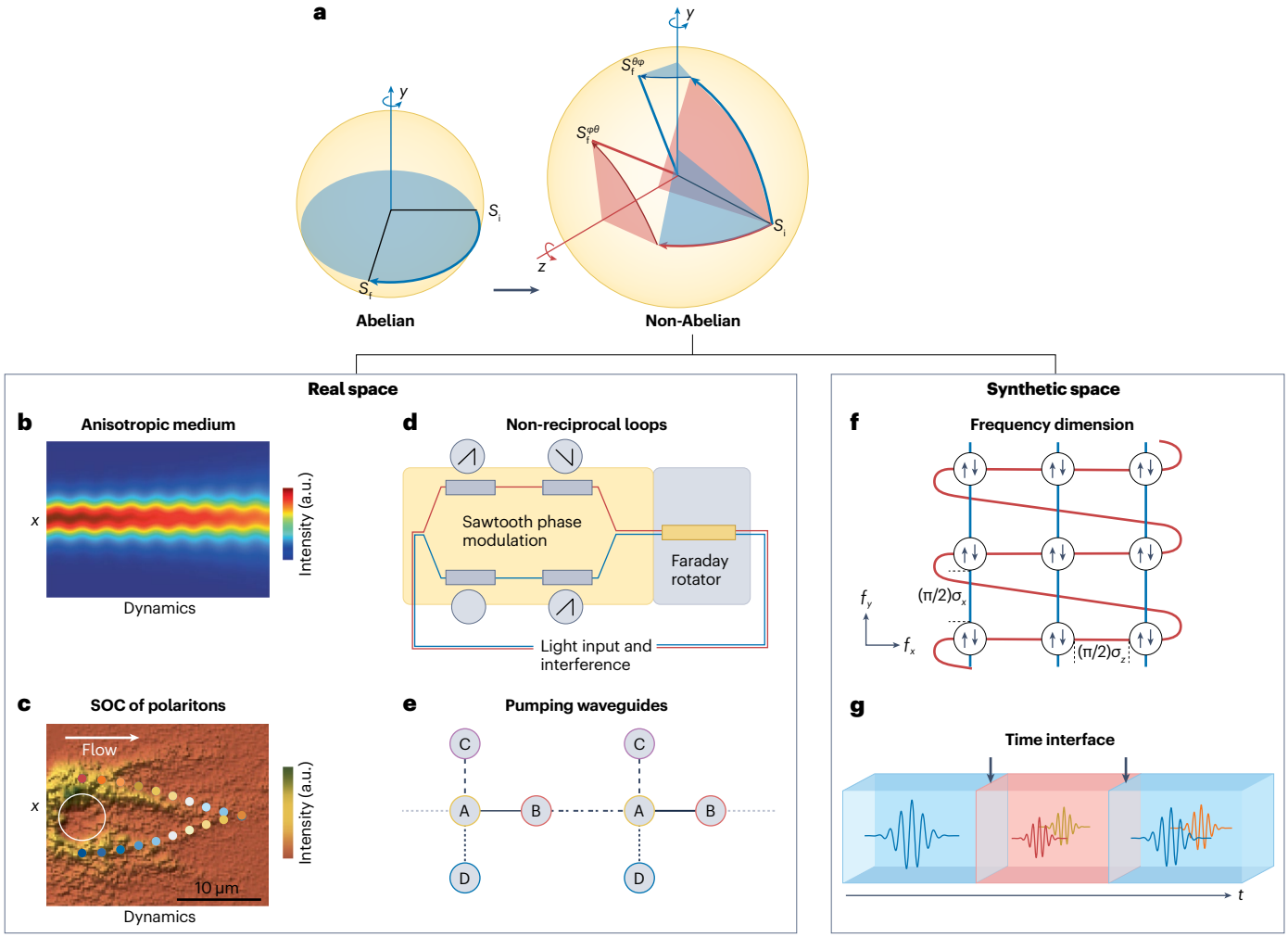

Fig. 4 | Non-Abelian gauge fields. a, In Abelian gauge fields (left panel), the states (S) in Hilbert space form a unit circle, and all rotations commute. In contrast, in non-Abelian SU(2) gauge fields (right panel), the states in Hilbert space form a unit sphere, where different sequences of the transformations result in different final states S_f (ref. 83). **b**, Zitterbewegung effect of optical beams in homogeneous anisotropic medium with synthetic non-Abelian magnetic field[86]. **c**, Non-Abelian lensing effect caused by a defect (white circle) embedded in a perovskite microcavity[87]. **d**, Non-reciprocal optical fibre loops generate non-Abelian Aharonov–Bohm interference[83]. **e**, Schematics for realizing non-Abelian Thouless pumping in waveguides arranged in a Lieb lattice configuration[93]. **f**, Non-Abelian lattice gauge fields in a 2D synthetic frequency lattice. f_x and f_y represent the two synthetic frequency axes[96]. **g**, Illustration of a temporal multilayer structure for 3D non-Abelian gauge field, where a wave traverses a discrete system, encountering two time interfaces at different times[98]. SOC, spin–orbit coupling. Part **a** adapted with permission from ref. 83, AAAS. Part **b** reprinted from ref. 86, Springer Nature Limited. Part **c** reprinted with permission from ref. 87, Optica. Part **d** adapted with permission from ref. 18, AAAS. Part **e** reprinted with permission from ref. 93, APS. Part **f** reprinted from ref. 96, Springer Nature Limited. Part **g** reprinted from ref. 98, Springer Nature Limited.

been proposed and demonstrated in waveguide systems, illustrating the non-Abelian effects by transforming an initial state into distinct final states through a sequence of operations[93] (Fig. 4e).

The construction of non-Abelian gauge fields in photonic systems is still a rapidly developing field, for which we direct the reader to two contemporary reviews on non-Abelian gauge field[18,94]. Currently, there are few experimental demonstrations of non-Abelian gauge fields in real-space photonic lattices. One of the challenges lies in introducing non-Abelian terms described by Pauli matrices into the lattice coupling. Unlike the asymmetric couplings in VGPs, non-Abelian gauge potentials require asymmetric couplings for both polarization states simultaneously. Inspired by the synthesis of non-Abelian gauge fields through non-reciprocal loops in real space[83], it is possible to introduce phase modulators and optical rotators in coupled ring resonators with synthetic dimensions. In this context, a 2D lattice of ring resonators that includes both a real spatial dimension and a synthetic spectral dimension enables the implementation of arbitrary SU(2) lattice gauge fields for photons[95], as recently experimentally confirmed through linear band crossings at the Dirac cones and the associated direction reversal of eigenstate trajectories[96] (Fig. 4f).

With the help of synthetic frequency dimensions, both synthetic Abelian and non-Abelian electric fields can be generated,

allowing the observation of the interplay between Bloch oscillations and Zitterbewegung through pulse dynamics[97]. Furthermore, the introduction of synthetic dimensions overcomes the limitations imposed by 3D spatial dimensions, making it possible to implement artificial non-Abelian gauge fields in higher dimensions. For instance, a temporal multilayer structure has been proposed to create *N*-dimensional non-Abelian gauge fields in a space including the time dimension[98] (Fig. 4g). This proposal involves several flexible operations to connect discrete sites with designed hopping phases, which are accessible within synthetic dimensions. Additionally, synthetic non-Abelian gauge fields in polarization-multiplexed photonic mesh lattices, along with the time synthetic dimension, can be used to realize and control topological quantum walks[99].

Complex gauge fields

Both the SGPs and VGPs described above are real valued and manifest in Hermitian systems. Over the past decade, non-Hermitian photonics has garnered considerable interest[19,20], particularly in exploiting the non-Hermitian degeneracies known as exceptional points (EPs)[21,22]. Different forms of non-Hermiticity have been introduced, extending artificial gauge fields (both real and vector ones) to the complex realm (see Box 1).

Although non-Hermitian photonics focusing on EPs was investigated in 1955 in the context of light propagating in absorbing biaxial crystals[100], it was the discovery of PT symmetry[101] in 1998, showing that the eigenfrequencies of a system can remain real despite its non-Hermitian nature, that started the explosive growth of the field. Since then, non-Hermitian photonic systems with gain and loss have been widely explored and have inspired a plethora of studies and applications[19–22,102–104].

From the perspective of gauge fields, PT symmetry, characterized by a refractive index with an even real part (n_r) and an odd imaginary part (n_i), corresponds to a specific modulation of the complex scalar optical potential. It has been recognized that, in general, more flexible modulation of complex gauge potentials is possible, enabling the exploration of non-Hermitian physics beyond the realm of PT symmetry. Non-Hermitian degeneracies (EPs), characterized by the coalescence of both eigenvalues and eigenvectors, are widely identified and are core concepts in non-Hermitian systems (Fig. 5a). Unlike Hermitian degeneracies, non-Hermitian degeneracies can lead to eigenmode swapping[105–107] as well as acquiring a non-trivial Berry phase. Thus, dynamic encirclement of EPs results in a counterintuitive chiral state transfer, promising novel on-chip light routing[108] and laser configurations[109]. Moreover, imaginary scalar gauge potentials can be combined with real VGPs, which involves topological concepts and emerges as another field of study that focuses on the topology of complex non-Hermitian degeneracies[110,111]. For example, a Weyl exceptional ring forms when non-uniform loss is added into a photonic waveguide array[112] (Fig. 5b). In general, using various lattice symmetries and synthetic dimensions, one can create non-Hermitian degeneracies in distinct forms, including exceptional curves[113] and surfaces[114], volumes or even higher-order EP assemblies.

Another type of non-Hermiticity that has attracted great interest is the off-diagonal non-Hermiticity originating from asymmetric hoppings, where $|c_{mn}| \neq |c_{nm}|$, subjected to an imaginary vector potential (see Box 1). Tracing back to the Hatano–Nelson model in the 1990s[115], the imaginary gauge field induced by asymmetric couplings is found to induce a delocalization transition in the Anderson model. The imaginary gauge fields in non-Hermitian tight-binding lattices[116,117] have garnered considerable interest because of their unique topological features under open boundary conditions, specifically the phenomenon known as the non-Hermitian skin effect (NHSE)[23,24,118–120]. This effect is characterized by the accumulation of bulk states around the edges of a non-Hermitian lattice, which can be understood in the tight-binding model, as illustrated below. In the presence of imaginary gauge fields, light acquire an imaginary phase factor along their trajectory, which, rather than contributing to interference, modifies the light field amplitudes along their hopping direction. This results in directional attenuation or amplification, leading to exponential localization at the edges under open boundary conditions (Fig. 5c). It is worth noting that there are other interpretations of the emergence of the NHSE, including state coalescences at EPs and a point-gap topology characterized by energy windings.

The NHSE has been demonstrated on various photonic platforms, including optical fibre loops[121], quantum walks of photons[122] and microring resonator arrays[123]. These demonstrations span spatial dimensions as well as synthetic dimensions such as frequency or polarization. For example, the NHSE has been observed in optical fibre loops showing optical funnel behaviour, where the 1D discrete-time quantum walk of temporal pulses forms a synthetic lattice with asymmetric hopping terms realized by a beamsplitter[121]. The imaginary vector potentials induced by asymmetric coupling are also interesting for laser design, for instance in the creation of topological bulk lasers[124] and robust phase-locking in laser arrays[125]. A coupled laser system can also generate an imaginary gauge field[126,127]. To circumvent the difficulty of realizing asymmetric couplings, the NHSE can be indirectly generated and controlled with the help of other types of artificial gauge fields and by using a proposed gain–loss scheme (that is, using imaginary scalar potentials) that breaks certain symmetries[128]. By adjusting the coupling phases in optical rings through assistant rings, the NHSE can be engineered by real vector gauge fields[129]. Moreover, the Floquet NHSE[130,131] has been demonstrated in an optical waveguide array by controlling the interplay between loss (imaginary scalar potentials) and the coupling phases (real vector potentials) induced by the Floquet engineering. In a Floquet system, the spatial modulation frequency allows one to engineer the NHSE topology. As shown in Fig. 5d, this approach has enabled a topological transition of the NHSE from unipolar to bipolar and broadband light funnelling in silicon photonics[132].

There is also an emerging branch of research that focuses on the joint effects of complex gauge potentials and non-Abelian gauge fields. Non-Hermitian systems with complex eigenvalues and non-orthogonal eigenvectors offer a new platform to investigate non-Abelian gauge phenomena. The geometry of non-Hermitian spectral manifolds, such as self-intersecting complex Riemann surfaces, serves as a natural testbed for non-Abelian braids. Single-band or two-band knots have been demonstrated in synthetic platforms using ring resonators[133], and multiband non-Abelian braids have been observed in cavity optomechanics[134]. Additionally, the interplay between complex gauge potentials and non-Abelian gauge fields has been studied, for example, by exploring non-Abelian effects in non-Hermitian systems characterized by non-conservative couplings[135]. This line of enquiry highlights that dissipation can lead to non-Abelian dynamics, characterized by non-commutative operators acting on the Bloch eigenstates[135] (Fig. 5e). In addition to these non-Hermiticity induced non-Abelian effects, non-Abelian gauge fields can also give rise to non-Hermitian phenomena. It has been found that even in 1D without gauge flux, non-Abelian gauge fields can induce rich non-Hermitian topological

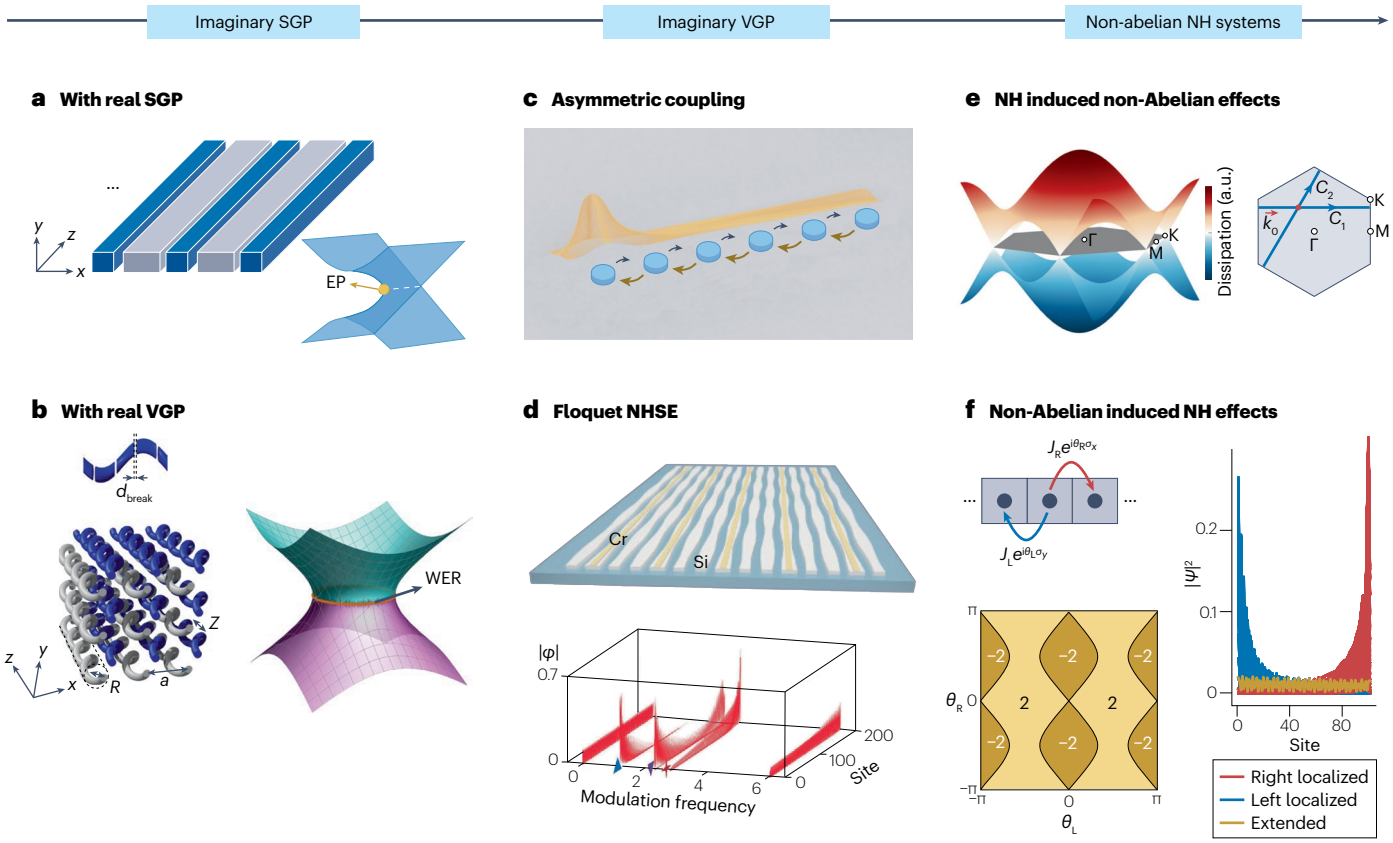

Fig. 5 | Complex gauge potentials. a, Schematic of an optical waveguide array with a transverse variation of both real scalar potentials (indicated by the waveguide width) and imaginary scalar potentials (indicated by the waveguide colour). The inset shows the energy surfaces of a non-Hermitian degeneracy (EP)[109]. **b**, A non-Hermitian Weyl exceptional ring (WER, right panel) in a lossy photonic helical waveguide array (left panel), where R, a, Z and d_{break} are structure parameters. Loss is introduced by interrupting the waveguides, characterized by parameter d_{break} (ref. 112). **c**, Schematic of exponentially localized skin modes with asymmetric couplings in a 1D lattice model[24]. **d**, Without asymmetric coupling, the non-Hermitian skin effect (NHSE; bottom panel) can be realized by Floquet modulation with coexisting real gauge field (by modulating the width of waveguides) and loss (introduced by a chromium stripe). The top panel illustrates the schematics of the implementation in silicon waveguides[132]. **e**, Non-Abelian dynamics involving Bloch eigenstates in a dissipative honeycomb lattice. Left, dissipation bands of the lattice Bloch eigenstates. Right, Brillouin zone with two distinct closed loops, C_1 and C_2, along which the initial state is transported[135]. **f**, Non-Abelian gauge fields in Hatano–Nelson models (top left) and the corresponding phase diagram (bottom left), where black solid lines indicate the emergence of exceptional points, resulting in the presence of the NHSE[136]. NH, non-Hermitian; SGP, scalar gauge potential; VGP, vector gauge potential. Part **a** adapted with permission from ref. 22, AAAS. Part **b** adapted from ref. 112, Springer Nature Limited. Part **c** is reprinted from ref. 24, CC BY 4.0. Part **d** adapted with permission from ref. 132, APS. Part **e** adapted from ref. 135, Springer Nature Limited. Part **f** reprinted with permission from ref. 136, APS.

phenomena, such as the simultaneous presence of non-Hermitian skin modes[136] (Fig. 5f). We anticipate that a more intricate interplay between non-Hermiticity and non-Abelian gauge fields will emerge in future research.

Non-Hermitian photonics has already been extensively reviewed[19–22,24,102–104] and often does not need to rely on the concept of complex potentials. Here, we focus on a few representative investigations for which the perspective of complex potentials either greatly simplifies the explanations or provides a clearer physical picture. As gauge potentials constitute a shared common language across different disciplines of physics[4], an alternative interpretation based on gauge potentials is not redundant. Instead, it can more effectively bridge optics and other fields of physics, which can and do inspire each other.

Artificial gauge fields for quantum electrodynamics

As with classical light waves, introducing artificial gauge fields into quantum photonic systems provides new opportunities, particularly from the strong photon–photon correlation that can be induced by interaction between photons and quantum materials[137]. The interplay between photon–photon interaction and artificial gauge fields remains underexplored. As strongly interacting electrons in gauge fields give rise to fractional quantum Hall effects, one may expect similar effects from strongly correlated photons. However, as photons obey bosonic statistics, simulating quantum effects typical of fermionic systems requires nonlinearity or additional synthetic degrees of freedom[138].

One of the key ingredients for introducing artificial gauge fields to quantum photonics is strong photon–atom interaction. To achieve this,

one can confine photons in a cavity or waveguide coupled to (artificial) atomic ensembles, as studied in cavity or waveguide quantum electrodynamics (QED). The (artificial) atoms can be ultracold atoms, molecules, quantum dots or superconducting qubits. Unlike real atoms, in which the same quantum states cannot be doubly occupied, superconducting qubits can be excited by two or more photons with anharmonic potentials. Storing photons in these superconducting circuits has led to the field of circuit QED[139]. One can further introduce artificial gauge fields and explore collective effects of photon–photon interaction in cavity, waveguide and circuit QEDs, realizing Laughlin states of light[25], photonic fractional quantum Hall states[138] and quantum topology of light[26].

One example of artificial gauge fields of photons and bosonic polaritons was realized in a twisted four-mirror cavity (Fig. 6a, left panel). In this configuration, the twist between resonators induces photon rotation about the optical axis, subjecting the photons to an artificial gauge field[25,140]. As a result, synthetic Landau levels of photons with different angular momenta can be observed in this system[140]. On further incorporating Rydberg atoms into the cavity, injected photons that carry orbital angular momentum excite polaritons in the lowest Landau level, enabling interactions between them. This process results in the emission of Laughlin states of light from the cavity[25,141] (Fig. 6a, right panel). The collisions of long-lived Rydberg polaritons play important roles in generating fractional quantum Hall states of light, as another paradigmatic example of topology. More generally, polaritons can be induced by strong coupling between quantum well excitations and microcavity photons, and applying perpendicular electric and magnetic fields can generate artificial gauge fields[142]. Furthermore, when the electrons are initially in the fractional quantum Hall regime, polariton–polariton interaction can be enhanced through the formation of polaron-polaritons to induce nonlinear responses of light[143]. We expect such strong polariton–polariton interactions to enable further many-body states of photons.

In waveguide QED systems (Fig. 6b), photons can assist long-range hopping of excitations from one atom to another. The photon-mediated hopping contains a phase factor that is determined by the hopping distance[144]. Because reverse hopping over the same distance adopts the same phase factor, the effective Hamiltonian of the excitation is non-Hermitian, and scale-free edge states exist due to radiative decay of excitation at the boundaries[145]. The dispersion diagram of such systems has disconnected branches, which prohibits the application of topological band theory. However, the inverse of the effective Hamiltonian gives a continuous inverse energy band, which can be used to define topological invariants[145].

In dimerized atomic arrays with inverse symmetry, one can find topological phases of the inverse band structure that changes with frequency and modulation phase. The scale-free localized states appear in only one inverse band for the topological phase but in both inverse bands for the trivial phase, which is different from conventional bulk-edge correspondence. In trimerized atomic arrays with two excitations, the modulation phase can provide an additional synthetic dimension, and the topological band with a non-trivial Chern number in the expanded 2D space can support topological bound edge states.

By connecting two arrays with the same artificial gauge field but different modulated phases, localized subradiant states appear on the interface[146]. Even in a simple array without any modulation, one extended excitation provides background potential for the other excitation. The momentum of the extended excitation plays the role of an effective magnetic field, which induces Landau levels and topological edge states of the other excitation[147].

In circuit QED systems, one can realize an artificial gauge field of photons in a ring of three qubits by sinusoidally modulating the

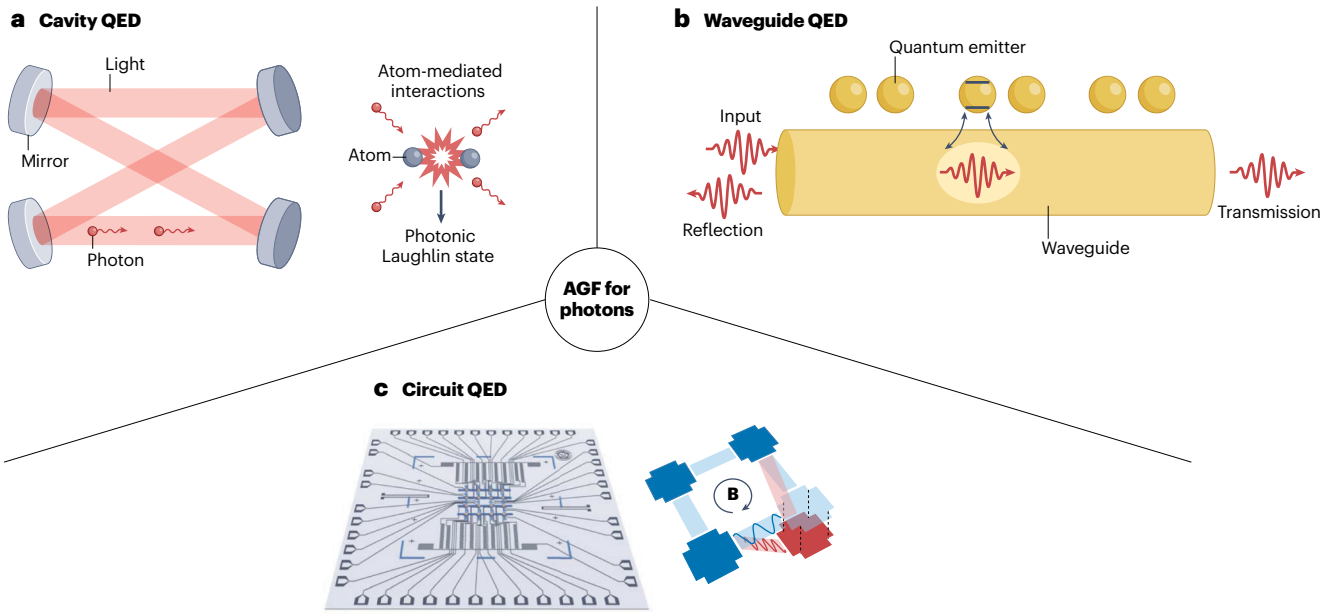

Fig. 6 | Artificial gauge fields for photons. a, Schematic of photons that interact with Rydberg atoms in a cavity consisting of four mirrors to form a photonic Laughlin state[141]. **b**, Schematic diagram of photonic scattering in waveguide quantum electrodynamics (QED)[145]. Photons propagating in the waveguide are scattered by quantum emitters precisely positioned along its length. **c**, Schematics of programmable on-chip platform based on circuit QED with artificial gauge field (AGF)[138]. Part **a** adapted from ref. 141, Springer Nature Limited. Part **b** reprinted with permission from ref. 145, APS. Part **c** adapted with permission from ref. 138, AAAS.

hopping strength[148]. As microwave photons can exhibit strong interactions, chiral ground states of photons have been observed in experiments, paving the way for the realization of fractional quantum Hall states. Recently, by using a programmable on-chip platform of circuit QED, an artificial gauge field has been realized in a much larger square lattice[138] (Fig. 6c). The ground state can be prepared by adiabatically ramping up the hopping strength and decreasing the potential differences. The correlation function and density current of the ground fractional Hall states have been measured, showing anti-bunching behaviours as a result of photon blockade and chiral density currents. Furthermore, the response of fractional quantum Hall states to the external field has been observed, including the incompressibility of generated quasiparticles and the characteristic signature of fractional quantum Hall conductivity. The measured ratio of bulk density of photons to magnetic flux is consistent with the ideal value of half of the Hall conductivity.

By modulating both onsite potentials and hopping strengths in a 1D qubit array, time-reversal symmetry is broken to support topological Thouless pumping, as a dynamical version of the quantum Hall effect. Strongly correlated Thouless pumping of photons has been demonstrated in a circuit QED system, showcasing topologically resonant tunnelling effects, in which two photons are shifted either as a whole or one by one[149,150]. Apart from the spatial dimension, the photon number can encode quantum information. In superconducting circuits, precise control over photon populations in individual resonators and their coupling strengths enables the construction of Fock-state lattices with artificial gauge field[26], thereby extending topological states of light into the quantum regime.

Challenges and further applications

Although considerable progress has been made in realizing artificial gauge fields across various physical systems, direct experimental demonstrations are still challenging for systems with sophisticated gauge field distributions. Key challenges include the precise control over system parameters, the stability of the generated fields, and the scalability of the experimental setups. These hurdles stem from technical constraints such as imperfections in lattice structures, decoherence effects and limitations in current manipulation techniques. For example, imaginary gauge fields obtained through active and/or dissipative media face technological challenges of lifetime broadening and noise, which inevitably compromise the robustness of the topological band structure. Furthermore, for practical photonic applications, effects of different sorts of nonlinearities and non-equilibrium have to be considered, as they can induce dynamical symmetry breaking and instability. Addressing these challenges necessitates the development of more advanced nanofabrication technologies[151,152] and dynamically reconfigurable platforms[96,153]. In addition, interdisciplinary efforts that blend insights from condensed matter physics, quantum information science and materials science could pave the way for new solutions. By tackling these experimental challenges head-on, one can advance the field to unlock the full potential of artificial gauge fields for practical applications.

One promising application on the horizon is for integrated photonic circuits — a rapidly advancing platform that is revolutionizing sensing, communication, optical computing, augmented and virtual reality, and other technologies. Several proof-of-concept demonstrations relying on artificial gauge fields have already been implemented in an integrated form[151–154], showing exceptional capabilities that had been believed inaccessible. For example, on-chip light routing based on artificial gauge fields offers higher robustness, density and flexibility than traditional methods[151]. In this context, ultra-broadband low-crosstalk transmissions in dense thin-film lithium niobate waveguides have been achieved through the Floquet-engineering of SGPs[154], providing an alternative solution for high-density on-chip photonic integrations. Additionally, artificial vector gauge fields enable dispersion control over coupler devices[151], overcoming traditional obstacles related to coupling efficiency, operational bandwidth and sensitivity to structural deviations, thereby enabling scaling to larger circuits. Another example of a dispersion-control device is related to the Landau rainbow[155], which has been realized through the combined operations of scalar and vector potentials. This approach aids in the design of slow-light devices and multiwavelength multiplexing devices that are robust, scalable and have broadband capability. The complex-valued vector potential, when applied to a waveguide, is able to enhance the optical force by an order of magnitude in integrated switches and actuators[156]. Beyond these tangible aspects, artificial gauge fields also have the potential to stimulate new applications in quantum photonics, enabling robust generation[157], transport[158], and interference of quantum photonic states[159], which are delicate and vulnerable to fabrication imperfections.

Although most proposals and demonstrations are still far from being widely used for technological applications, some implementations[151–159] have already enhanced the performance of optical components that are indispensable for applications inaccessible to traditional techniques. Going forward, functionalities relying on artificial gauge fields can substantially improve photonic components of waveguides, couplers, routers, cavities, filters, delay-line devices, circulators, isolators, lasers, sensors, directional emitters and more. Further assisted by exotic materials (such as low-dimensional, quasiperiodic and fractal structures) and artificial intelligence[160–162], artificial gauge field photonic devices may function as the backbone of many disruptive technologies, such as robust optical communication systems[152,153], topological quantum computing[157–159] and neuromorphic photonic circuits[160].

Published online: 16 September 2025

References

1. Yang, C. N. in *Selected Papers of Chen Ning Yang II*, 78–92 (World Scientific, 2013).
2. Aidelsburger, M., Nascimbene, S. & Goldman, N. Artificial gauge fields in materials and engineered systems. *C. R. Phys.* **19**, 394–432 (2018).
3. Aharonov, Y. & Bohm, D. Significance of electromagnetic potentials in the quantum theory. *Phys. Rev.* **115**, 485–491 (1959).
4. Wu, T. T. & Yang, C. N. Concept of nonintegrable phase factors and global formulation of gauge fields. *Phys. Rev. D* **12**, 3845–3857 (1975).
5. Madison, K. W., Chevy, F., Wohlleben, W. & Dalibard, J. Vortex formation in a stirred Bose–Einstein condensate. *Phys. Rev. Lett.* **84**, 806–809 (2000).
6. Lin, Y. J., Compton, R. L., Jiménez-García, K., Porto, J. V. & Spielman, I. B. Synthetic magnetic fields for ultracold neutral atoms. *Nature* **462**, 628–632 (2009).
7. Fang, K., Yu, Z. & Fan, S. Realizing effective magnetic field for photons by controlling the phase of dynamic modulation. *Nat. Photon.* **6**, 782–787 (2012).
8. Rechtsman, M. C. et al. Photonic floquet topological insulators. *Nature* **496**, 196–200 (2013).
   Experimental realizations of photonic Floquet topological insulators.
9. Fang, K. J. et al. Generalized non-reciprocity in an optomechanical circuit via synthetic magnetism and reservoir engineering. *Nat. Phys.* **13**, 465–471 (2017).
10. Süsstrunk, R. & Huber, S. D. Observation of phononic helical edge states in a mechanical topological insulator. *Science* **349**, 47–50 (2015).
11. Xiao, M., Chen, W.-J., He, W.-Y. & Chan, C. T. Synthetic gauge flux and Weyl points in acoustic systems. *Nat. Phys.* **11**, 920–924 (2015).
12. Lee, C. H. et al. Topolectrical circuits. *Commun. Phys.* **1**, 39 (2018).
13. Pendry, J. B., Schurig, D. & Smith, D. R. Controlling electromagnetic fields. *Science* **312**, 1780–1782 (2006).
    Introducing the concept of transformation optics, providing a blueprint for designing materials that can precisely control the path of electromagnetic fields.

14. Miri, M. A., Heinrich, M., El-Ganainy, R. & Christodoulides, D. N. Supersymmetric optical structures. *Phys. Rev. Lett.* **110**, 233902 (2013).
15. Lu, L., Joannopoulos, J. D. & Soljačić, M. Topological photonics. *Nat. Photon.* **8**, 821–829 (2014).
16. Ozawa, T. et al. Topological photonics. *Rev. Mod. Phys.* **91**, 015006 (2019).
Comprehensive review of recent advances in topological photonics.
17. Zhang, X., Zangeneh-Nejad, F., Chen, Z.-G., Lu, M.-H. & Christensen, J. A second wave of topological phenomena in photonics and acoustics. *Nature* **618**, 687–697 (2023).
18. Yang, Y. et al. Non-Abelian physics in light and sound. *Science* **383**, 844 (2024).
19. Feng, L., El-Ganainy, R. & Ge, L. Non-Hermitian photonics based on parity–time symmetry. *Nat. Photon.* **11**, 752–762 (2017).
20. El-Ganainy, R. et al. Non-Hermitian physics and PT symmetry. *Nat. Phys.* **14**, 11–19 (2018).
21. Özdemir, S. K., Rotter, S., Nori, F. & Yang, L. Parity–time symmetry and exceptional points in photonics. *Nat. Mater.* **18**, 783–798 (2019).
22. Miri, M.-A. & Alù, A. Exceptional points in optics and photonics. *Science* **363**, eaar7709 (2019).
23. Yao, S. Y. & Wang, Z. Edge states and topological invariants of non-Hermitian systems. *Phys. Rev. Lett.* **121**, 086803 (2018).
Extension of topological band theory to non-Hermitian system.
24. Zhang, X., Zhang, T., Lu, M.-H. & Chen, Y.-F. A review on non-Hermitian skin effect. *Adv. Phys.: X* **7**, 2109431 (2022).
25. Clark, L. W., Schine, N., Baum, C., Jia, N. Y. & Simon, J. Observation of Laughlin states made of light. *Nature* **582**, 41–45 (2020).
26. Deng, J. F. et al. Observing the quantum topology of light. *Science* **378**, 966–971 (2022).
Experimental observation of quantum topological properties of light.
27. Huang, K. *Fundamental Forces of Nature: The Story of Gauge Fields* (World Scientific, 2007).
28. Bloch, F. Uber die Quantenmechanik der Elektronen in Kristallgittern. *Z. Phys. A* **52**, 555–600 (1928).
29. Zener, C. A theory of the electrical breakdown of solid dielectrics. *Proc. R. Soc. Lond. A* **145**, 523–529 (1934).
30. Peschel, U., Pertsch, T. & Lederer, F. Optical Bloch oscillations in waveguide arrays. *Opt. Lett.* **23**, 1701–1703 (1998).
31. Block, A. et al. Bloch oscillations in plasmonic waveguide arrays. *Nat. Commun.* **5**, 3843 (2014).
32. Liu, W., Neshev, D. N., Miroshnichenko, A. E., Shadrivov, I. V. & Kivshar, Y. S. Bouncing plasmonic waves in half-parabolic potentials. *Phys. Rev. A* **84**, 063805 (2011).
33. Levy, U. et al. Inhomogenous dielectric metamaterials with space-variant polarizability. *Phys. Rev. Lett.* **98**, 243901 (2007).
34. Staliunas, K. & Masoller, C. Subdiffractive light in bi-periodic arrays of modulated fibers. *Opt. Express* **14**, 10669–10677 (2006).
35. Pyrialakos, G. G. et al. Bimorphic Floquet topological insulators. *Nat. Mater.* **21**, 634–639 (2022).
36. Hwang, M.-S., Kim, H.-R. & Park, H.-G. Topological manipulation for advancing nanophotonics. *npj Nanophoton.* **1**, 32 (2024).
37. Peterson, C. W. et al. Trapped fractional charges at bulk defects in topological insulators. *Nature* **589**, 376–380 (2021).
38. Liu, Y. et al. Bulk-disclination correspondence in topological crystalline insulators. *Nature* **589**, 381–385 (2021).
39. Hu, Z. et al. Topological orbital angular momentum extraction and twofold protection of vortex transport. *Nat. Photon.* **19**, 162–169 (2025).
40. Yang, Z., Lustig, E., Lumer, Y. & Segev, M. Photonic Floquet topological insulators in a fractal lattice. *Light Sci. Appl.* **9**, 128 (2020).
41. Biesenthal, T. et al. Fractal photonic topological insulators. *Science* **376**, 1114–1119 (2022).
42. Miri, M. A., Heinrich, M. & Christodoulides, D. N. SUSY-inspired one-dimensional transformation optics. *Optica* **1**, 89–95 (2014).
43. Yim, J. et al. Broadband continuous supersymmetric transformation: a new paradigm for transformation optics. *eLight* **2**, 16 (2022).
44. Hokmabadi, M. P., Nye, N. S., El-Ganainy, R., Christodoulides, D. N. & Khajavikhan, M. Supersymmetric laser arrays. *Science* **363**, 623–626 (2019).
45. Heinrich, M. et al. Supersymmetric mode converters. *Nat. Commun.* **5**, 3698 (2014).
46. Liu, X. et al. Perfect excitation of topological states by supersymmetric waveguides. *Phys. Rev. Lett.* **132**, 016601 (2024).
47. Vonklitzing, K., Dorda, G. & Pepper, M. New method for high-accuracy determination of the fine-structure constant based on quantized hall resistance. *Phys. Rev. Lett.* **45**, 494–497 (1980).
48. Onoda, M., Murakami, S. & Nagaosa, N. Hall effect of light. *Phys. Rev. Lett.* **93**, 083901 (2004).
49. Haldane, F. D. M. & Raghu, S. Possible realization of directional optical waveguides in photonic crystals with broken time-reversal symmetry. *Phys. Rev. Lett.* **100**, 013904 (2008).
50. Wang, Z., Chong, Y. D., Joannopoulos, J. D. & Soljacic, M. Observation of unidirectional backscattering-immune topological electromagnetic states. *Nature* **461**, 772–775 (2009).
51. Rechtsman, M. C. et al. Strain induced pseudomagnetic field and photonic Landau levels in dielectric structures. *Nat. Photon.* **7**, 153–158 (2013).
52. Yang, Z., Gao, F., Yang, Y. & Zhang, B. Strain-induced gauge field and Landau levels in acoustic structures. *Phys. Rev. Lett.* **118**, 194301 (2017).
53. Huang, Z. T. et al. Pattern-tunable synthetic gauge fields in topological photonic graphene. *Nanophotonics* **11**, 1297–1308 (2022).
54. Hafezi, M., Mittal, S., Fan, J., Migdall, A. & Taylor, J. M. Imaging topological edge states in silicon photonics. *Nat. Photon.* **7**, 1001–1005 (2013).
55. Wu, L. H. & Hu, X. Scheme for achieving a topological photonic crystal by using dielectric material. *Phys. Rev. Lett.* **114**, 223901 (2015).
56. Dong, J. W., Chen, X. D., Zhu, H. Y., Wang, Y. & Zhang, X. Valley photonic crystals for control of spin and topology. *Nat. Mater.* **16**, 298–302 (2017).
57. Gao, F. et al. Topologically protected refraction of robust kink states in valley photonic crystals. *Nat. Phys.* **14**, 140–144 (2018).
58. Fang, K., Yu, Z. & Fan, S. Photonic Aharonov–Bohm effect based on dynamic modulation. *Phys. Rev. Lett.* **108**, 153901 (2012).
59. Luo, H. K. et al. Guiding Trojan light beams via Lagrange points. *Nat. Phys.* **20**, 95–100 (2024).
60. Celi, A. et al. Synthetic gauge fields in synthetic dimensions. *Phys. Rev. Lett.* **112**, 043001 (2014).
61. Yu, D. et al. Comprehensive review on developments of synthetic dimensions. *Photon. Insights* **4**, R06–R06 (2025).
62. Yuan, L., Shi, Y. & Fan, S. Photonic gauge potential in a system with a synthetic frequency dimension. *Opt. Lett.* **41**, 741 (2016).
63. Lustig, E. et al. Photonic topological insulator in synthetic dimensions. *Nature* **567**, 356–360 (2019).
64. Wimmer, M., Price, H. M., Carusotto, I. & Peschel, U. Experimental measurement of the Berry curvature from anomalous transport. *Nat. Phys.* **13**, 545–550 (2017).
65. Luo, X. W. et al. Synthetic lattice enabled all-optical devices based on orbital angular momentum of light. *Nat. Commun.* **8**, 16097 (2017).
66. Dutt, A. et al. A single photonic cavity with two independent physical synthetic dimensions. *Science* **367**, 59–64 (2020).
Exploration of higher-dimensional physics using synthetic dimensions.
67. Citro, R. & Aidelsburger, M. Thouless pumping and topology. *Nat. Rev. Phys.* **5**, 87–101 (2023).
68. Zilberberg, O. et al. Photonic topological boundary pumping as a probe of 4D quantum Hall physics. *Nature* **553**, 59–62 (2018).
69. Wang, Q., Xiao, M., Liu, H., Zhu, S. N. & Chan, C. T. Optical interface states protected by synthetic Weyl points. *Phys. Rev. X* **7**, 031032 (2017).
70. Song, W. et al. Bound-extended mode transition in type-II synthetic photonic Weyl heterostructures. *Phys. Rev. Lett.* **132**, 143801 (2024).
71. Ozawa, T., Price, H. M., Goldman, N., Zilberberg, O. & Carusotto, I. Synthetic dimensions in integrated photonics: from optical isolation to four-dimensional quantum Hall physics. *Phys. Rev. A* **93**, 043827 (2016).
72. Ma, S. et al. Linked Weyl surfaces and Weyl arcs in photonic metamaterials. *Science* **373**, 572–576 (2021).
73. Yang, Y. et al. Demonstration of negative refraction induced by synthetic gauge fields. *Sci. Adv.* **7**, eabj2062 (2021).
74. Lumer, Y. et al. Light guiding by artificial gauge fields. *Nat. Photon.* **13**, 339–345 (2019).
Illustrating how artificial gauge fields can be used to control light in photonic structures.
75. Pilozzi, L., Leykam, D., Chen, Z. & Conti, C. Topological photonic crystal fibers and ring resonators. *Opt. Lett.* **45**, 1415–1418 (2020).
76. Zhu, B. et al. Topological photonic crystal fibre. Preprint at https://arxiv.org/abs/2501.15107 (2025).
77. Niu, Q. et al. Realization of a Dirac-vortex topological photonic crystal fiber. Preprint at https://arxiv.org/abs/2503.04194 (2025).
78. Song, W. et al. Subwavelength self-imaging in cascaded waveguide arrays. *Adv. Photon.* **2**, 036001 (2020).
79. Pendry, J. B. Negative refraction makes a perfect lens. *Phys. Rev. Lett.* **85**, 3966 (2000).
80. Ye, H. et al. Reconfigurable refraction manipulation at synthetic temporal interfaces with scalar and vector gauge potentials. *Proc. Natl Acad. Sci. USA* **120**, e2300860120 (2023).
81. Wang, S. L. et al. High-order dynamic localization and tunable temporal cloaking in ac-electric-field driven synthetic lattices. *Nat. Commun.* **13**, 7653 (2022).
82. Wang, S. et al. Photonic Floquet Landau–Zener tunneling and temporal beam splitters. *Sci. Adv.* **9**, eadh0415 (2023).
83. Yang, Y. et al. Synthesis and observation of non-Abelian gauge fields in real space. *Science* **365**, 1021–1025 (2019).
Realizing the synthesis and observation of non-Abelian gauge fields in real space.
84. Arnold, V. *Lectures and Problems: A Gift to Young Mathematicians* (American Math Society (translated from Russian), 2015).
85. Yang, C. N. & Mills, R. L. Conservation of isotopic spin and isotopic gauge invariance. *Phys. Rev.* **96**, 191–195 (1954).
86. Chen, Y. et al. Non-Abelian gauge field optics. *Nat. Commun.* **10**, 3125 (2019).
87. Polimeno, L. et al. Experimental investigation of a non-Abelian gauge field in 2D perovskite photonic platform. *Optica* **8**, 1442–1447 (2021).
88. Lovett, S. et al. Observation of Zitterbewegung in photonic microcavities. *Light Sci. Appl.* **12**, 126 (2023).
89. Ye, W. et al. Photonic Hall effect and helical Zitterbewegung in a synthetic Weyl system. *Light Sci. Appl.* **8**, 49 (2019).
90. Wu, J. et al. Non-Abelian gauge fields in circuit systems. *Nat. Electron.* **5**, 635–642 (2022).
91. Terças, H., Flayac, H., Solnyshkov, D. D. & Malpuech, G. Non-Abelian gauge fields in photonic cavities and photonic superfluids. *Phys. Rev. Lett.* **112**, 066402 (2014).
92. Whittaker, C. E. et al. Optical analogue of Dresselhaus spin–orbit interaction in photonic graphene. *Nat. Photon.* **15**, 193–196 (2021).

93. Brosco, V., Pilozzi, L., Fazio, R. & Conti, C. Non-Abelian Thouless pumping in a photonic lattice. *Phys. Rev. A* **103**, 063518 (2021).
94. Yan, Q. et al. Non-Abelian gauge field in optics. *Adv. Opt. Photon.* **15**, 907–976 (2023).
95. Cheng, D. L., Wang, K. & Fan, S. H. Artificial non-Abelian lattice gauge fields for photons in the synthetic frequency dimension. *Phys. Rev. Lett.* **130**, 083601 (2023).
96. Cheng, D. et al. Non-Abelian lattice gauge fields in photonic synthetic frequency dimensions. *Nature* **637**, 52–56 (2025).
97. Wong, B. T. T., Yang, S., Pang, Z. & Yang, Y. Synthetic non-Abelian electric fields and spin–orbit coupling in photonic synthetic dimensions. *Phys. Rev. Lett.* **134**, 163803 (2025).
98. Dong, Z. et al. Temporal multilayer structures in discrete physical systems towards arbitrary-dimensional non-Abelian Aharonov–Bohm interferences. *Nat. Commun.* **15**, 7392 (2024).
99. Pang, Z., Abdelghani, O., Soljačić, M. & Yang, Y. Topological quantum walk in synthetic non-Abelian gauge fields. Preprint at https://arxiv.org/abs/2412.03043 (2024).
100. Pancharatnam, S. The propagation of light in absorbing biaxial crystals. *Proc. Indian Acad. Sci. A* **42**, 86–109 (1955).
101. Bender, C. M. & Boettcher, S. Real spectra in non-Hermitian Hamiltonians having PT symmetry. *Phys. Rev. Lett.* **80**, 5243 (1998).
102. Li, A. D. et al. Exceptional points and non-Hermitian photonics at the nanoscale. *Nat. Nanotechnol.* **18**, 706–720 (2023).
103. Ding, K., Fang, C. & Ma, G. C. Non-Hermitian topology and exceptional-point geometries. *Nat. Rev. Phys.* **4**, 745–760 (2022).
104. Wang, C. Q. et al. Non-Hermitian optics and photonics: from classical to quantum. *Adv. Opt. Photon.* **15**, 442–523 (2023).
105. Doppler, J. et al. Dynamically encircling an exceptional point for asymmetric mode switching. *Nature* **537**, 76–79 (2016).
Encircling an exceptional point for asymmetric mode switching.
106. Nasari, H. et al. Observation of chiral state transfer without encircling an exceptional point. *Nature* **605**, 256–261 (2022).
107. Song, W. G. et al. Breakup and recovery of topological zero modes in finite non-Hermitian optical lattices. *Phys. Rev. Lett.* **123**, 165701 (2019).
108. Li, A. D. et al. Hamiltonian hopping for efficient chiral mode switching in encircling exceptional points. *Phys. Rev. Lett.* **125**, 187403 (2020).
109. Schumer, A. et al. Topological modes in a laser cavity through exceptional state transfer. *Science* **375**, 884–888 (2022).
110. Zhen, B. et al. Spawning rings of exceptional points out of Dirac cones. *Nature* **525**, 354–358 (2015).
111. Zhou, H. et al. Observation of bulk Fermi arc and polarization half charge from paired exceptional points. *Science* **359**, 1009–1012 (2018).
112. Cerjan, A. et al. Experimental realization of a Weyl exceptional ring. *Nat. Photon.* **13**, 623–628 (2019).
113. Song, W. et al. Observation of Weyl interface states in non-Hermitian synthetic photonic systems. *Phys. Rev. Lett.* **130**, 043803 (2023).
114. Zhang, X., Ding, K., Zhou, X., Xu, J. & Jin, D. Experimental observation of an exceptional surface in synthetic dimensions with magnon polaritons. *Phys. Rev. Lett.* **123**, 237202 (2019).
115. Hatano, N. & Nelson, D. R. Localization transitions in non-Hermitian quantum mechanics. *Phys. Rev. Lett.* **77**, 570–573 (1996).
116. Sun, C.-P. High-order adiabatic approximation for non-Hermitian quantum system and complexification of Berry's phase. *Phys. Scr.* **48**, 393 (1993).
117. Longhi, S., Gatti, D. & Valle, G. D. Non-Hermitian transparency and one-way transport in low dimensional lattices by an imaginary gauge field. *Phys. Rev. B* **92**, 094204 (2015).
118. Okuma, N., Kawabata, K., Shiozaki, K. & Sato, M. Topological origin of non-Hermitian skin effects. *Phys. Rev. Lett.* **124**, 086801 (2020).
119. Zhang, K., Yang, Z. S. & Fang, C. Correspondence between winding numbers and skin modes in non-Hermitian systems. *Phys. Rev. Lett.* **125**, 126402 (2020).
120. Borgnia, D. S., Kruchkov, A. J. & Slager, R. J. Non-Hermitian boundary modes and topology. *Phys. Rev. Lett.* **124**, 056802 (2020).
121. Weidemann, S. et al. Topological funneling of light. *Science* **368**, 311–314 (2020).
Experimental realization of the non-Hermitian skin effect.
122. Xiao, L. et al. Non-Hermitian bulk boundary correspondence in quantum dynamics. *Nat. Phys.* **16**, 761–766 (2020).
123. Xin, H. R. et al. Manipulating the non-Hermitian skin effect in optical ring resonators. *Phys. Rev. B* **107**, 165401 (2023).
124. Longhi, S. Non-Hermitian gauged topological laser arrays. *Ann. Phys.* **530**, 1800023 (2018).
125. Teo, W. X., Zhu, W. W. & Gong, J. B. Tunable two-dimensional laser arrays with zero-phase locking. *Phys. Rev. B* **105**, L201402 (2022).
126. Liu, Y. G. N. et al. Complex skin modes in non-Hermitian coupled laser arrays. *Light Sci. Appl.* **11**, 336 (2022).
127. Gao, Z. H. et al. Two dimensional reconfigurable non-Hermitian gauged laser array. *Phys. Rev. Lett.* **130**, 263801 (2023).
128. Yi, Y. F. & Yang, Z. S. Non-Hermitian skin modes induced by on-site dissipations and chiral tunneling effect. *Phys. Rev. Lett.* **125**, 186802 (2020).
129. Lin, Z. K., Ding, L., Ke, S. L. & Li, X. Steering non-Hermitian skin modes by synthetic gauge fields in optical ring resonators. *Opt. Lett.* **46**, 3512–3515 (2021).
130. Li, Y., Lu, C., Zhang, S. & Liu, Y.-C. Loss-induced Floquet non-Hermitian skin effect. *Phys. Rev. B* **108**, L220301 (2023).
131. Sun, Y. et al. Photonic Floquet skin-topological effect. *Phys. Rev. Lett.* **132**, 063804 (2023).
132. Lin, Z. et al. Observation of topological transition in Floquet non-Hermitian skin effects in silicon photonics. *Phys. Rev. Lett.* **133**, 073803 (2024).
133. Wang, K., Dutt, A., Wojcik, C. C. & Fan, S. Topological complex energy braiding of non-Hermitian bands. *Nature* **598**, 59–64 (2021).
134. Patil, Y. S. S. et al. Measuring the knot of non-Hermitian degeneracies and non-commuting braids. *Nature* **607**, 271–275 (2022).
135. Parto, M., Leefmans, C., Williams, J., Nori, F. & Marandi, A. Non-Abelian effects in dissipative photonic topological lattices. *Nat. Commun.* **14**, 1440 (2023).
136. Pang, Z., Wong, B. T. T., Hu, J. & Yang, Y. Synthetic non-Abelian gauge fields for non-Hermitian systems. *Phys. Rev. Lett.* **132**, 043804 (2024).
137. Shen, J. T. & Fan, S. H. Strongly correlated two-photon transport in a one-dimensional waveguide coupled to a two-level system. *Phys. Rev. Lett.* **98**, 153003 (2007).
138. Wang, C. et al. Realization of fractional quantum Hall state with interacting photons. *Science* **384**, 579–584 (2024).
Realizing the optical simulation of fractional quantum Hall physics.
139. Blais, A., Grimsmo, A. L., Girvin, S. M. & Wallraff, A. Circuit quantum electrodynamics. *Rev. Mod. Phys.* **93**, 025005 (2021).
140. Schine, N., Ryou, A., Gromov, A., Sommer, A. & Simon, J. Synthetic landau levels for photons. *Nature* **534**, 671–675 (2016).
141. Corman, L. Light turned into exotic Laughlin matter. *Nature* **582**, 37–38 (2020).
142. Lim, H. T., Togan, E., Kroner, M., Miguel-Sanchez, J. & Imamoglu, A. Electrically tunable artificial gauge potential for polaritons. *Nat. Commun.* **8**, 14540 (2017).
143. Knüppel, P. et al. Nonlinear optics in the fractional quantum Hall regime. *Nature* **572**, 91–94 (2019).
144. Ke, Y. G., Poshakinskiy, A. V., Lee, C. H., Kivshar, Y. S. & Poddubny, A. N. Inelastic scattering of photon pairs in qubit arrays with subradiant states. *Phys. Rev. Lett.* **123**, 253601 (2019).
145. Ke, Y. G., Huang, J. X., Liu, W. J., Kivshar, Y. S. & Lee, C. H. Topological inverse band theory in waveguide quantum electrodynamics. *Phys. Rev. Lett.* **131**, 103604 (2023).
146. Ke, Y. G. et al. Radiative topological biphoton states in modulated qubit arrays. *Phys. Rev. Res.* **2**, 033190 (2020).
147. Poshakinskiy, A. V. et al. Quantum Hall phases emerging from atom–photon interactions. *npj Quantum Inf.* **7**, 3435 (2021).
148. Roushan, P. et al. Chiral ground-state currents of interacting photons in a synthetic magnetic field. *Nat. Phys.* **13**, 146–151 (2017).
149. Walter, A.-S. et al. Quantization and its breakdown in a Hubbard–Thouless pump. *Nat. Phys.* **19**, 1471–1475 (2023).
150. Ke, Y. & Lee, C. Topological quantum tango. *Nat. Phys.* **19**, 1387–1388 (2023).
151. Song, W. et al. Dispersionless coupling among optical waveguides by artificial gauge field. *Phys. Rev. Lett.* **129**, 053901 (2022).
Introducing artificial gauge fields into photonic chips for broadband optical coupling.
152. Feng, X. et al. Non-Hermitian hybrid silicon photonic switching. *Nat. Photon.* **19**, 264–270 (2025).
153. Dai, T. et al. A programmable topological photonic chip. *Nat. Mater.* **23**, 928–936 (2024).
154. Lin, Z. et al. Ultrabroadband low-crosstalk dense lithium niobate waveguides by Floquet engineering. *Phys. Rev. Appl.* **20**, 054005 (2023).
155. Zhao, W. et al. Landau rainbow induced by artificial gauge fields. *Phys. Rev. Lett.* **133**, 233801 (2024).
156. Descheemaeker, L., Ginis, V., Viaene, S. & Tassin, P. Optical force enhancement using an imaginary vector potential for photons. *Phys. Rev. Lett.* **119**, 137402 (2017).
157. Mittal, S., Goldschmidt, E. A. & Hafezi, M. A topological source of quantum light. *Nature* **561**, 502–506 (2018).
158. Blanco-Redondo, A., Bell, B., Oren, D., Eggleton, B. J. & Segev, M. Topological protection of biphoton states. *Science* **362**, 568–571 (2018).
159. Tambasco, J.-L. et al. Quantum interference of topological states of light. *Sci. Adv.* **4**, 3187 (2018).
160. Wang, Z. et al. Artificial-gauge-field-based inverse design for wideband-flat power splitter and microring resonator. *Adv. Photon. Nexus* **4**, 016001 (2025).
161. Pilozzi, L., Farrelly, F. A., Marcucci, G. & Conti, C. Machine learning inverse problem for topological photonics. *Commun. Phys.* **1**, 57 (2018).
162. Xia, S. et al. Deep-learning-empowered synthetic dimension dynamics: morphing of light into topological modes. *Adv. Photon.* **6**, 026005 (2024).

Acknowledgements

The authors thank all their collaborators on the topic of artificial gauge fields and related work. W.S. and T.L. acknowledge funding from the National Key R&D Program of China (2023YFA1407700, 2022YFA1404301) and National Natural Science Foundation of China (nos. 12522421, 12204233, 12174186, 62288101, 92250304 and 62325504). W.L. is supported by Outstanding Young Researcher Scheme of Hunan Province (2024JJ2056). S.Z. acknowledges support from the Quantum Science Center of Guangdong–Hong Kong–Macau Great Bay Area, New Cornerstone Science Foundation and the Hong Kong Research Grant Council (STG3/E-704/23-N, AoE/P-701/20, 17315522).

Author contributions

All authors researched data for the article. All authors contributed substantially to discussion of the content. All authors wrote the article. W.S., W.L., Y.K., T.L. and S.Zhang reviewed and/or edited the manuscript before submission.

Competing interests
The authors declare no competing interests.

Additional information
Peer review information *Nature Reviews Physics* thanks the anonymous reviewers for their contribution to the peer review of this work.

Publisher's note Springer Nature remains neutral with regard to jurisdictional claims in published maps and institutional affiliations.